Accepted Manuscript

Thermal photogrammetric imaging: A new technique for monitoring dome eruptions

Samuel T. Thiele, Nick Varley, Mike R. James

Please cite this article as: Samuel T. Thiele, Nick Varley, Mike R. James , Thermal photogrammetric imaging: A new technique for monitoring dome eruptions. The address for the corresponding author was captured as affiliation for all authors. Please check if appropriate. Volgeo(2017), doi: 10.1016/j.jvolgeores.2017.03.022

Thermal Photogrammetric Imaging: A New Technique for Monitoring Dome Eruptions

Samuel T. Thiele[a,b*], Nick Varley[a] & Mike R. James[c]

[a]Colima Intercambio e Investigación en Vulcanología, Universidad de Colima, av. Universidad 333, Las Viboras C.P. 28040, Colima, México

[b]School of Earth, Atmosphere and Environment, Monash University, Clayton VIC 3800, Australia

[c]Lancaster Environment Centre, Lancaster University, Lancaster LA1 4YQ, UK

*Corresponding Author: sam.thiele01@gmail.com

Abstract

Structure-from-motion (SfM) algorithms greatly facilitate the generation of 3-D topographic models from photographs and can form a valuable component of hazard monitoring at active volcanic domes. However, model generation from visible imagery can be prevented due to poor lighting conditions or surface obscuration by degassing. Here, we show that thermal images can be used in a SfM workflow to mitigate these issues and provide more continuous time-series data than visible counterparts. We demonstrate our methodology by producing georeferenced photogrammetric models from 30 near-monthly overflights of the lava dome that formed at Volcán de Colima (Mexico) between 2013 and 2015. Comparison of thermal models with equivalents generated from visible-light photographs from a consumer digital single lens reflex (DSLR) camera suggests that, despite being less detailed than their DSLR counterparts, the thermal models are more than adequate reconstructions of dome geometry, giving volume estimates within 10% of those derived using the DSLR.

Significantly, we were able to construct thermal models in situations where degassing and poor lighting prevented the construction of models from DSLR imagery, providing substantially better data continuity than would have otherwise been possible. We conclude that thermal photogrammetry provides a useful new tool for monitoring effusive volcanic activity and assessing associated volcanic risks.

Key words: Lava Dome, Photogrammetry, Thermal Imaging, Volcán de Colima

1. Introduction

Lava domes are known to pose significant volcanic hazards, due to their tendency to generate collapse related pyroclastic flows and their association with explosive eruptions (Fink and Anderson, 2000). For example, successive dome collapses at Soufrière Hills on the island of Montserrat, starting in 1995, caused the evacuation and eventual abandonment of the capital Plymouth and surrounding areas (Wadge et al., 2014), while the 1994 collapse of Mount Merapi (Indonesia) resulted in 95 deaths and damage to several villages (Abdurachman et al., 2000). A similar event at Volcán de Colima in 2015 generated pyroclastic flows that travelled ~10 km, fortunately causing only minor damage.

Monitoring of dome geometry (e.g. volume and height), growth rate and deformation is key to forecasting such dome collapse events (Voight, 2000), and photogrammetry and structure from motion (SfM) are increasingly being used for this purpose (e.g. Herd et al., 2005; Ryan et al., 2010; Diefenbach et al., 2012; James and Varley, 2012; Diefenbach et al., 2013). Using these techniques, morphological and geometric data can be safely and inexpensively acquired, and used to track eruption progress, identify signs of instability or changes in effusion rate, and forecast changes in volcanic risk. These methods, however, rely on clear viewing conditions and so are highly sensitive to degassing, cloud and poor lighting conditions.

Thermal imaging techniques are also widely used for monitoring purposes (Spampinato et al., 2011), as they allow quantitative evaluation of heat flux from volcanic vents (e.g. Harris and Stevenson, 1997; Sahetapy-Engel et al., 2008), domes (e.g. Hutchison et al., 2013; Pallister et al., 2013), flows (e.g. Calvari et al., 2003; James et al., 2006) and fumaroles (e.g. Stevenson and Varley, 2008; Harris et al., 2009). Importantly, the spatial distribution of heat flux can reveal features that are difficult to detect using reflected visible light, such as fumaroles, fractures and rock fall traces (Hutchison et al., 2013; Mueller et al., 2013).

Changes in the distribution and intensity of thermal anomalies can also precede volcanic eruptions or changes in eruptive style (Spampinato et al., 2011) and thus have potential for hazard forecasting. However, to facilitate inter-survey comparisons, thermal data need to be spatially referenced, and producing orthorectified thermal maps usually requires additional topographic data, knowledge of the camera location and viewing direction (e.g. James et al., 2006; James et al., 2009; Lewis et al., 2015).

This study demonstrates a method for deriving topographic data and georeferenced thermal maps directly from oblique thermal imagery using SfM techniques and imagery captured during an episode of dome growth at Volcán de Colima (Mexico) between 2013 and 2015. We suggest that the resulting three-dimensional thermal models provide intuitive and georeferenced representations of dome surface temperature and valuable measurements of dome geometry. Furthermore, we demonstrate that despite the lower spatial resolution of thermal images, dome volume estimates are comparable to those estimated using SfM reconstructions deriving from visible-light digital single lens reflex (DSLR) photographs, and that unlike the DSLR models, the thermal models can be constructed during periods of poor lighting and extensive degassing.

Volcán de Colima is an andesitic and frequently erupting stratovolcano, located at the western limit of the Trans-Mexican Volcanic Belt. During the most recent eruptive periods, six episodes of dome growth have been observed at the volcano (1998–1999, 2001–2003, 2004, 2007–2011, 2013–2015

and an ongoing episode initiated in February 2016). This represents the most active period at the volcano since its last catastrophic eruption in 1913. A range of effusion rates have been estimated, with the longer-lived eruptions associated with rates as low as 0.01 m^3 s^{-1}. During the current eruption the volcano has exhibited the continuous generation of small Vulcanian explosions with a frequency of the order of hours. Larger magnitude explosions usually follow periods of dome emplacement, which re-excavate the summit crater.

The episode of dome growth investigated in this study began in January 2013 when lava erupted into the base of a ~150 m wide and ~50 m deep crater formed (by several large explosions that same month) on top of a previous (2007 to 2011) lava dome. The new dome proceeded to fill this crater and by April 2013 overflowed to form several lava flows and eventually fill the entire summit crater (~300 m across). Several partial collapses (accompanied by increased volcanic activity) resulted in dome destruction on 10 – 11 July 2015; pyroclastic density currents generated by these collapses travelled up to ~10.6 km along the ravine of Montegrande, threatening several ranches and the town of Quesaría (pop. 8611 in 2010). This eruption was the largest (by volume) at Volcán de Colima since 1913.

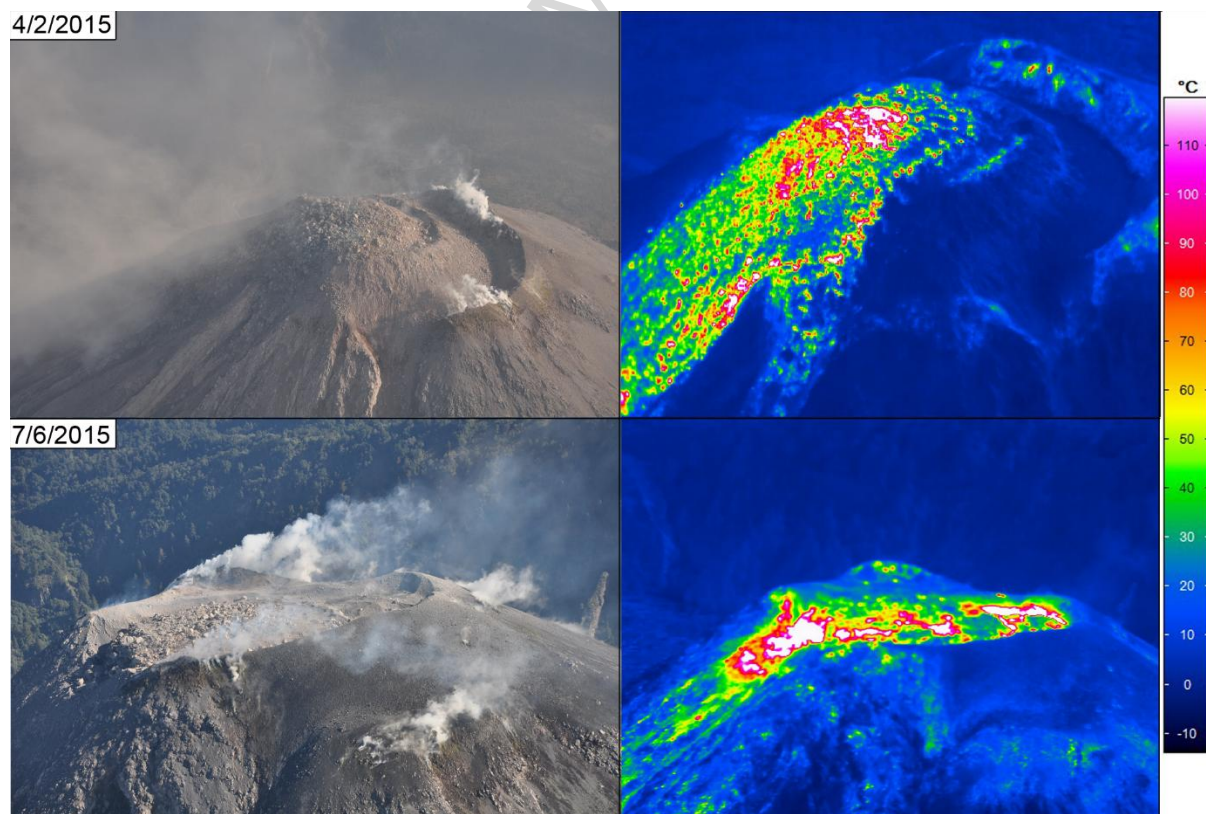## 2. Methods

2.1. Image capture and pre-processing

Images (Fig. 1) were acquired using a consumer DSLR (Nikon D90) and a thermal camera (Jenoptik VarioCAM HiRes) from a light aircraft during 30 observation flights, conducted at intervals of approximately one month. The DSLR had an 18–105 mm zoom lens (most images were captured using the 105 mm setting), while the thermal camera used a 75 mm fixed-focal lens. Thermal images had an order of magnitude lower resolution than the DSLR images (640×480 pixels and 4288×2848 pixels respectively).

Observational flights involved 2–3 circuits around the crater at a slightly higher elevation than the summit. Typical viewing distances varied between ~1–3 km, corresponding to ground sampling

distances of ~5-15 cm/pixel for the DSLR camera (at full zoom) and ~25-75 cm/pixel for the thermal camera. Both cameras were operated by hand, with DSLR photographs captured every ~5–10 seconds and the thermal camera programmed to take an image every 3.5 seconds.

Blurry and poorly exposed images were manually removed from the resulting image sets (of ~100 DSLR images and ~200–400 thermal images) prior to photogrammetric processing. Normally, ~50–75 DSLR images and ~100–200 thermal images were considered usable, though this varied substantially with viewing conditions.

The thermal images were converted from Jenoptic's proprietary IRB format to JPEG (using a colour scale selected to maximise the amount of detail visible on the dome and volcanic flanks) before photogrammetric processing. A second set of JPEG images were additionally created from the thermal images using a fixed colour scale, and later projected onto the photogrammetric model to create a thermal texture map that can be compared between models.

Figure 1. Examples of typical DSLR (left) and thermal (right) images from two different observation flights. Both views are looking to the north-west, and the summit region is ~300 m across.

2.2. Structure from Motion

Photogrammetric processing of both the DSLR and thermal datasets was performed using Agisoft Photoscan Professional Edition (v1.2.3). Prior to 3D reconstruction, both photosets were masked to remove degassing plumes, aircraft parts and unnecessary background, ensuring that only the edifice region was reconstructed. SfM methods were applied to estimate camera locations, orientations and internal parameters and produce a 'sparse point cloud' containing the location of tens of thousands of automatically detected features. These data were then used to constrain a detailed reconstruction of the volcanic edifice, producing a 'dense point cloud' (typically containing 10 – 20 million points for the DSLR models and ~0.5 million points for the thermal models).

Finally, a continuous triangulated surface model was derived from the dense point cloud for image rendering. For practical reasons, we limited the model to 1 million triangles, prior to texturing by projecting the original images onto its surface. For the thermal models, the photoset used to construct the model was exchanged with the photoset with a consistent colour-scale prior to the texturing step.

2.3. Georeferencing and Alignment

Due to difficult access and high risk, ground control points were not available for any of the models. Instead, similar to the approach used by James and Varley (2012), models generated from the DSLR images were georeferenced (within Agisoft Photoscan) by minimising the distance between features identified on the models and equivalent features located in Google Earth imagery. Here, we additionally used 1-arc second SRTM (Shuttle Radar Topographic Mission) data from February 2000 to derive elevations. As the morphology of the summit area changed substantially over the study period, it was necessary to use Google Earth imagery from different dates for some models, causing

relative translations of the results (reflecting the georeferencing error within Google Earth; coordinates of some static features changed by >20 meters between imagery from different dates).

To improve the registration between models and facilitate direct comparisons, the relative georeferencing of each model was optimised by aligning to one reference model (from 11 January 2013) using the iterative closest point (ICP) alignment implementation in Cloud Compare (Girardeau-Montaut, 2015). Model location, orientation and scale was allowed to vary during this step, during which areas known to have changed (i.e. the dome and associated flows) were manually excluded.

Models constructed using thermal images could not generally be georeferenced from the Google Earth imagery due to difficulties identifying corresponding features in the thermal data. Instead, they were aligned to the DSLR model from the same flight (or from a previous flight if the DSLR model had failed), using a manual 3-D point-matching approach in Meshlab (Cignoni et al., 2008) to achieve an initial alignment that was then optimised using ICP.

Where possible, the similarity (and alignment) of the DSLR and thermal models was assessed by comparison with DSLR models generated from the same flight. As the ICP alignment algorithm only applies a scaling and rigid body transformation, similarities between the DSLR and thermal models suggest that the photogrammetric reconstructions converge on a consistent surface shape, adding confidence to the results. Note that while this assessment provides an indication of uncertainty in the overall model shapes, it cannot evaluate the full geospatial uncertainty because the thermal models are not independently georeferenced.
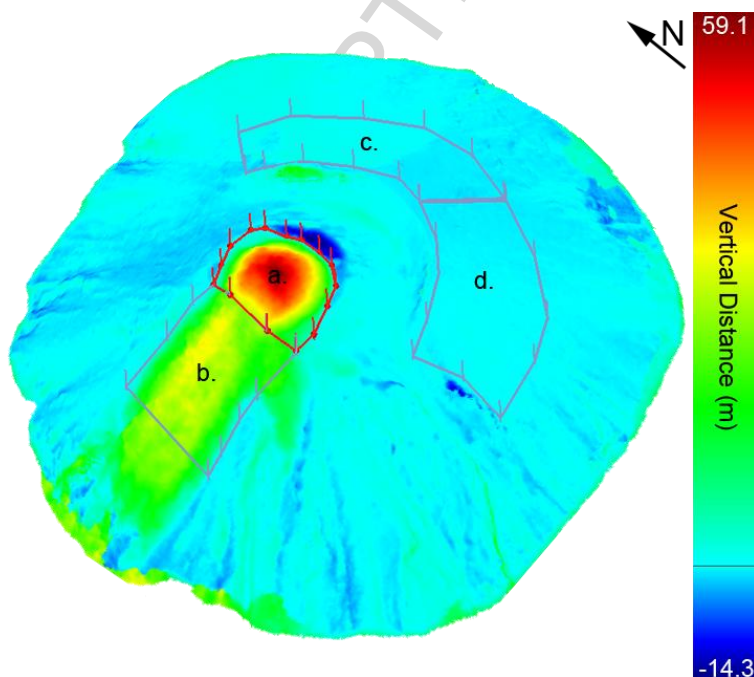
2.4. Volume Calculation

Dome volume was estimated by determining the difference between each photogrammetric model and the pre-dome reference model created photogrammetrically using data from a flight on 11 January 2013. The difference calculations (performed using a Java implementation of the signed tetrahedral method; Zhang and Chen, 2001) determined the volume between the surfaces in up to

four 'regions of interest' (ROI; Fig. 2). In this instance, a ROI containing the lava dome was defined for each of the photogrammetric models (both DSLR and thermal), and the volume of the dome estimated by comparison with a reference surface representing the pre-dome topography. Where the dome overflowed the crater (and transitioned into a lava flow), a consistent (but visually estimated) 'dome boundary' was defined (the boundary between regions a and b in Fig. 2), and the volume of the upper portion of a lava flow was also determined.

In order to better evaluate the uncertainty of the volume estimates, change within two stable reference areas on the flanks of the volcano was also calculated; because these areas should not vary, detecting volume change within them suggests greater uncertainty in the topographic models or their relative registration. These changes were expressed as mean vertical offsets that could then be used to estimate the dome volume (positive or negative) that likely resulted from alignment errors. Note however, that these reference areas were always located on the eastern flanks of the volcano, as the western flanks changed substantially over the study period (due to lava flows), and hence are not equally sensitive to all types of alignment error (e.g. translations or rotations) in dome area.

Figure 2: Oblique view of the 'regions of interest' defined for the 27/4/13 photogrammetric model. Region (a) contains the growing lava dome, and (b) the incipient lava flow. Regions (c) and (d) are the reference areas. The colour map represents the vertical distance between the comparison and reference surfaces. The dome region (a) is ~140 m across.

3. Results and Discussion

The 30 survey flights allowed the construction of 19 usable models from visible imagery and 22 models from the thermal imagery, although thermal data was only available for 23 flights. These datasets provide a reconstruction of the summit lava dome geometry at ~monthly intervals for the entire dome-forming eruption.

3.1. Comparison of Thermal and DSLR models

Both sets of photogrammetric models (thermal and DSLR) reconstructed the crater and dome complex on Volcán de Colima with varying degrees of completeness, detail and accuracy (Fig. 3). It is clear that, in general, models constructed using the thermal images were substantially less detailed than DSLR equivalents. This will be due to a combination of the thermal images having a lower spatial resolution than the DSLR images and a lack of high-frequency image texture, due to low thermal contrast on the volcano flanks.
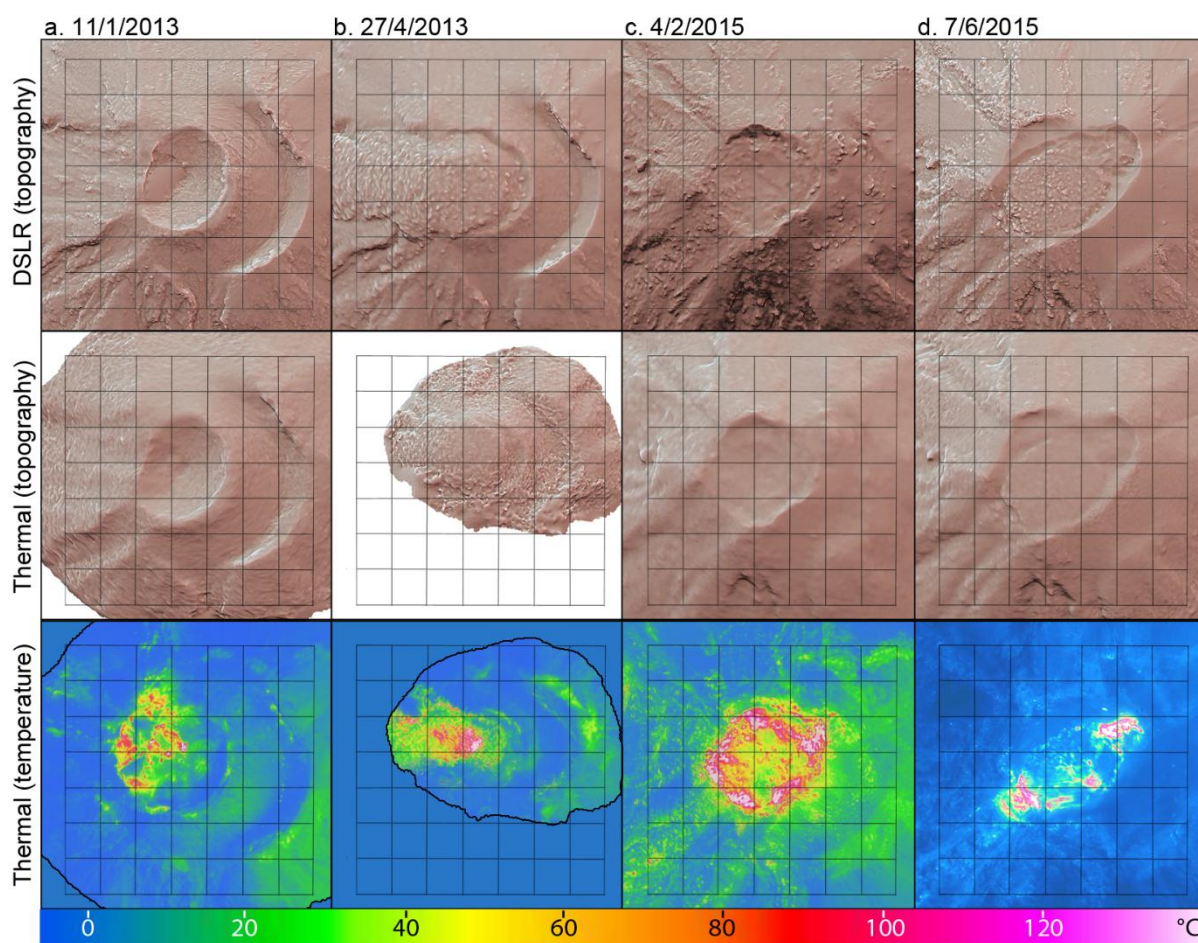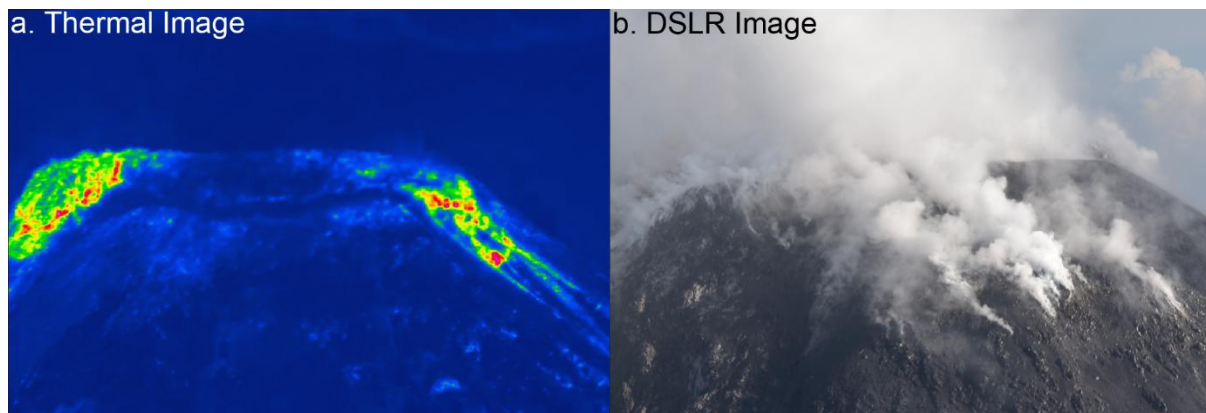
Figure 3. Selected DSLR and thermal photogrammetric models illustrated by hillshade (top and middle), and associated thermal orthomosaics (bottom). Grid cells are 50×50 m and oriented north-south and east-west. The model shown in (a) was captured before lava dome growth and was used as the reference model in volume calculations.

Nevertheless, 3D reconstruction using the thermal images was found to be far more robust to poor photography conditions than the DSLR models. In particular, thermal models could be constructed in situations where degassing made useful reconstruction from the DSLR images impossible. This is because water droplets in the degassing plume cause near complete scattering of visible light (and hence the plumes appear white), whilst the thermal infrared radiation (7.5-14 μm) is less affected (Fig. 4). Of all flights for which both thermal and DSLR data was available, ~30% of the DSLR surveys failed to generate a model while only ~5% of the thermal models failed, even though image locations and overlap were approximately the same. Hence, in addition to providing a useful map of estimated

temperature across the crater complex, the thermal models provide greater data continuity than the models from the DSLR.

Figure 4. Thermal (a) and DSLR (b) images captured at approximately the same time and location (looking towards the east), under strong degassing conditions. The dome is generally resolvable in the thermal image, but is substantially obscured in the DSLR image. A photogrammetric model of the dome was successfully reconstructed from the thermal images, and is of particular importance as it was captured on 5/7/15, days before the major July 2015 eruption. A model was not attempted using the DSLR data due to the degassing.

Shortest distance comparisons between associated DSLR and thermal models show generally good agreement (Fig. 5a and b). As thermal models tend to be smoother than the DSLR models (Fig. 3), differences tend to be focused around sharp topographic features such as the crater rim. However, in a few cases, the thermal models did differ significantly from their DSLR counterparts (Table 1). The largest dome volume difference was observed at the time when the dome area was largest (Fig. 5b), but the second largest observed dome volume difference resulted from the thermal model locating the dome surface ~5 m higher than the DSLR model (Fig. 5c). The reason for this difference is unclear, but highlights our ability to identify uncertainty by comparing the different datasets. A few of the thermal models also contained substantial error (±10 m; Fig. 5d), which was mostly apparent in areas of low thermal contrast, where image alignments and surface reconstructions are likely to

be weakest. Although the active lava surfaces were not directly influenced by this effect, the noisy

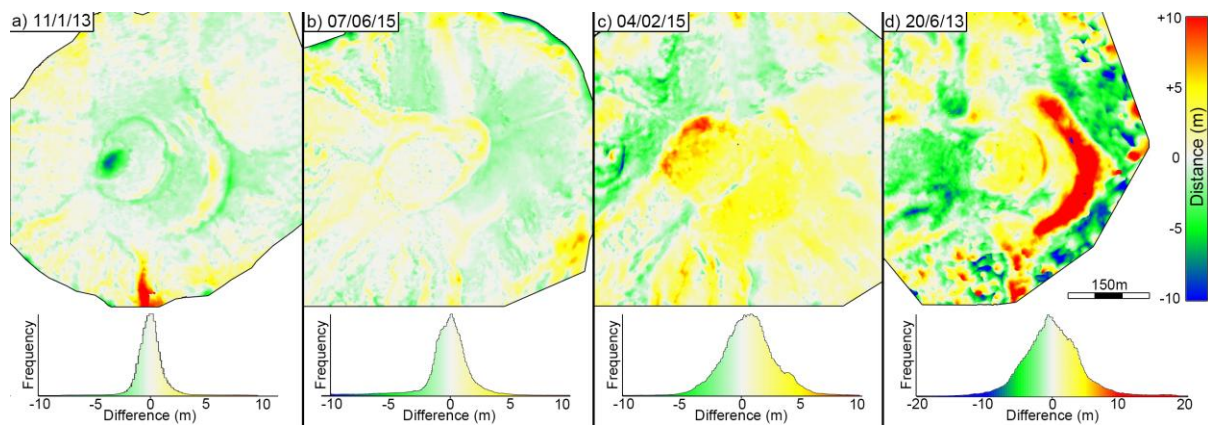surfaces did impair the ICP process and probably increased registration error.

Figure 5. The shortest distance between corresponding DSLR and thermal models. Regions where the thermal model is above the DSLR model are yellow-red, while areas where the DSLR model is on top are shaded green-blue. Histograms showing the distribution of the difference values are shown below each map. Examples of typical models are shown in (a) and (b), with few large differences except along sharp features (e.g. the crater rim) and towards model boundaries. Examples of models showing greater differences are presented in (c) and (d), where reconstructed dome geometries do not match well (c) or where substantial error is present (d).

Table 1: The five largest differences between the thermal and DSLR volume estimates. Volumes and differences are in million m^3. Percentages are relative to the DSLR volume estimate.

Model	DSLR Volume	Thermal Volume	Difference	% Difference
7/06/2015	1.16	1.05	0.11	9%
4/02/2015	1.10	1.20	0.10	9%
20/06/2013	0.51	0.56	0.05	9%
14/02/2014	0.51	0.55	0.04	7%
2/12/2013	0.54	0.52	0.02	3%

Using consumer cameras, and in the absence of ground control points sufficient to help constrain

photogrammetric processing, SfM-based data have been previously shown to provide topographic

data with an overall precision of ~1/1000 of the viewing distance (James and Robson, 2012). Thus,

over viewing distances of ~1-3 km, the 1-5 m differences between models are in line with this rule of thumb. These results are reasonable given the low resolution of the thermal camera and the relatively narrow angular field of view of both cameras (12° for the DSLR camera at full zoom and 10° for the thermal camera), which can cause difficulties for precise photogrammetric reconstruction. It is likely that the orbital flight paths play a strong role in helping to reduce error by naturally providing convergent imagery, which mitigates systematic model deformation effects when ground control points cannot be incorporated into the photogrammetric processing (Wackrow and Chandler, 2008; James and Robson, 2014).

3.2. Dome volume calculations

Dome volumes calculated independently using the DSLR and thermal models generally correspond well (Fig. 6), and differ by <10%. Likewise, the volume difference within the reference areas tended to be small, averaging 5% of the dome volume estimates.

While the volcanological significance and the implications of these results for understanding the 2013 – 2015 eruption are beyond the scope of this paper, it is clear that they provide valuable information on phases of dome growth (and volume loss) at Volcán de Colima between 2013 and 2015 (Fig. 6). Average effusion rates could also be estimated from the rate of dome volume change, although the effect of volume loss through explosive activity and lava flows would need to be accounted for.

Finally, where both DSLR and thermal models were successful, the two independent reconstructions also provide a valuable indication of uncertainty in model shape. Future studies could extend this approach and use GPS devices to "geotag" image locations at the time of capture, allowing additional evaluation of georeferencing uncertainty as the thermal models would no longer rely on ICP registration against a similar visible-light model for their georeferencing. For high quality camera position data, this 'direct georeferencing' approach has been shown capable of delivering decametric accuracies (Nolan et al., 2015). Alternatively, where sufficient topographic features are

recognisable in the thermal models, a single georeferenced model or high resolution digital elevation model of known accuracy could be used for georeferencing, avoiding the need for closely associated DSLR models.
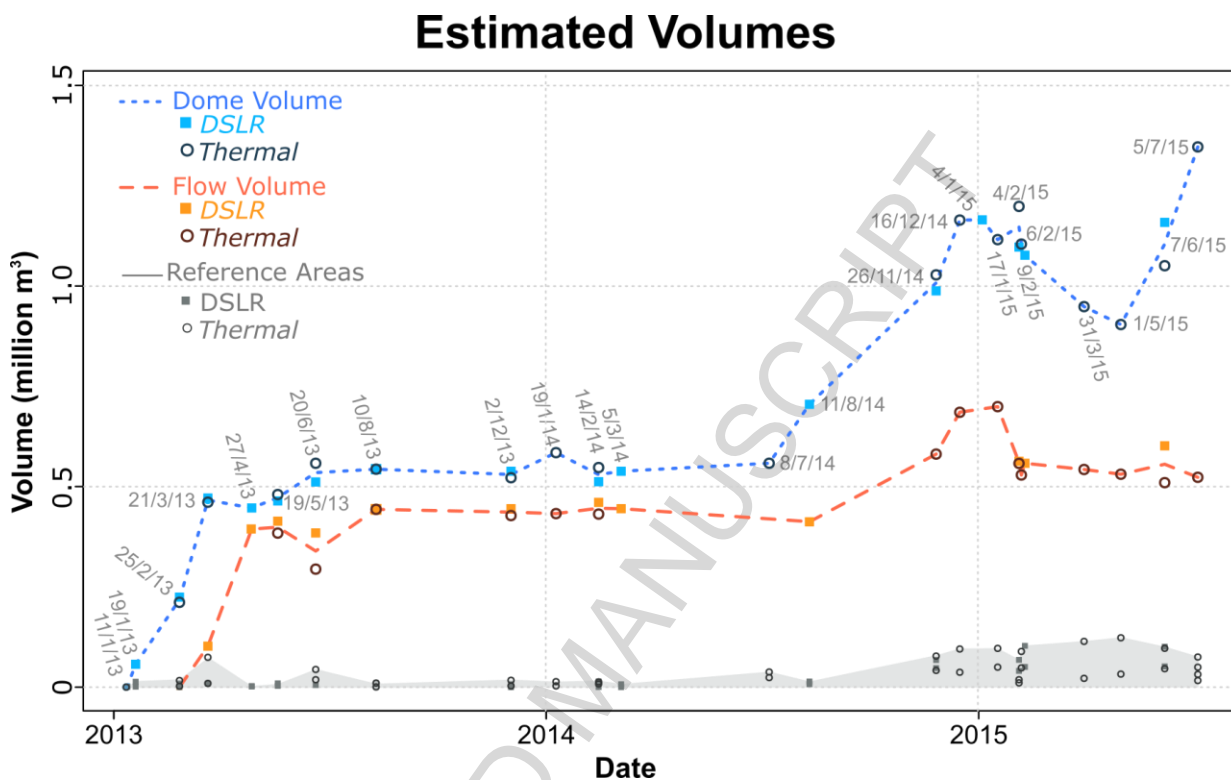

Figure 6. Volume of the lava dome (dotted) and lava flow top (dashed) between initiation of dome growth in January 2013 and dome collapse in July 2015. Where both DSLR (squares) and thermal (circles) models were available, the lines represent an average estimate. It is clear that there is generally good agreement between volumes calculated with the DSLR and thermal models. Reference area volumes (which would be zero under error-free conditions) are shown in grey to give an indication of relative accuracy.

4. Conclusions

We have successfully used SfM techniques and oblique thermal images to produce a time-series of georeferenced, three-dimensional thermal models of an active lava dome at Volcán de Colima. Comparisons between these models and equivalents derived from DSLR images suggest that, while

less detailed, the thermal models provide a valuable representation of dome geometry. Estimates of the lava dome volume correspond well between the DSLR and thermal datasets.

The thermal models were found to be substantially more robust to the adverse effects of degassing and poor lighting. Because degassing is common at Volcán de Colima (as at many other volcanoes) thermal imaging provided important data continuity at times when DSLR image quality was restricted. Where both DSLR and thermal models were available, the thermal models provided a useful complementary geometry estimate, helping to identify uncertainty in the models, and a georeferenced map of temperature distribution that allows identification of thermally active regions on the dome surface.

The combined DSLR and thermal datasets provided detailed information about the evolution of the dome on Volcán de Colima between 2013 and 2015. It is possible that, if employed as a monitoring technique (rather than retrospectively), the rapid change in dome volume, morphology and temperature distribution documented by the models in the months leading up to July 2015 may have provided prior warning of the dome collapse.

Acknowledgements

References

Abdurachman, E., Bourdier, J.-L., Voight, B., 2000. Nuées ardentes of 22 November 1994 at Merapi volcano, Java, Indonesia. Journal of Volcanology and Geothermal Research 100, 345-361.
Calvari, S., Neri, M., Pinkerton, H., 2003. Effusion rate estimations during the 1999 summit eruption on Mount Etna, and growth of two distinct lava flow fields. Journal of Volcanology and Geothermal Research 119, 107-123.
Cignoni, P., Corsini, M., Ranzuglia, G., 2008. Meshlab: an open-source 3d mesh processing system. Ercim news 73, 45-46.

Diefenbach, A.K., Bull, K.F., Wessels, R.L., McGimsey, R.G., 2013. Photogrammetric monitoring of lava dome growth during the 2009 eruption of Redoubt Volcano. Journal of Volcanology and Geothermal Research 259, 308-316. http://dx.doi.org/10.1016/j.jvolgeores.2011.12.009.

Diefenbach, A.K., Crider, J.G., Schilling, S.P., Dzurisin, D., 2012. Rapid, low-cost photogrammetry to monitor volcanic eruptions: an example from Mount St. Helens, Washington, USA. Bull Volcanol 74, 579-587.

Fink, J.H., Anderson, S.W., 2000. Lava domes and coulees. Encyclopedia of volcanoes, 307-319.

Girardeau-Montaut, D., 2015. Cloud Compare—3D Point Cloud and Mesh Processing Software. Open Source Project.

Harris, A.J., Lodato, L., Dehn, J., Spampinato, L., 2009. Thermal characterization of the Vulcano fumarole field. Bull Volcanol 71, 441-458.

Harris, A.J.L., Stevenson, D.S., 1997. Thermal observations of degassing open conduits and fumaroles at Stromboli and Vulcano using remotely sensed data. Journal of Volcanology and Geothermal Research 76, 175-198. http://dx.doi.org/10.1016/S0377-0273(96)00097-2.

Herd, R.A., Edmonds, M., Bass, V.A., 2005. Catastrophic lava dome failure at Soufrière Hills volcano, Montserrat, 12–13 July 2003. Journal of Volcanology and Geothermal Research 148, 234-252.

Hutchison, W., Varley, N., Pyle, D.M., Mather, T.A., Stevenson, J.A., 2013. Airborne thermal remote sensing of the Volcán de Colima (Mexico) lava dome from 2007 to 2010. Geological Society, London, Special Publications 380, 203-228.

James, M.R., Pinkerton, H., Applegarth, L.J., 2009. Detecting the development of active lava flow fields with a very-long-range terrestrial laser scanner and thermal imagery. Geophysical Research Letters 36. 10.1029/2009GL040701.

James, M.R., Robson, S., 2012. Straightforward reconstruction of 3D surfaces and topography with a camera: Accuracy and geoscience application. Journal of Geophysical Research 117. 10.1029/2011jf002289.

James, M.R., Robson, S., 2014. Mitigating systematic error in topographic models derived from UAV and ground-based image networks. Earth Surface Processes and Landforms 39, 1413-1420. 10.1002/esp.3609.

James, M.R., Robson, S., Pinkerton, H., Ball, M., 2006. Oblique photogrammetry with visible and thermal images of active lava flows. Bull Volcanol 69, 105-108. 10.1007/s00445-006-0062-9.

James, M.R., Varley, N., 2012. Identification of structural controls in an active lava dome with high resolution DEMs: Volcán de Colima, Mexico. Geophysical Research Letters 39. 10.1029/2012gl054245.

Lewis, A., Hilley, G.E., Lewicki, J.L., 2015. Integrated thermal infrared imaging and structure-from-motion photogrammetry to map apparent temperature and radiant hydrothermal heat flux at Mammoth Mountain, CA, USA. Journal of Volcanology and Geothermal Research 303, 16-24. http://dx.doi.org/10.1016/j.jvolgeores.2015.07.025.

Mueller, S., Varley, N., Kueppers, U., Lesage, P., Davila, G.Á.R., Dingwell, D.B., 2013. Quantification of magma ascent rate through rockfall monitoring at the growing/collapsing lava dome of Volcán de Colima, Mexico. Solid Earth 4, 201.

Nolan, M., Larsen, C., Sturm, M., 2015. Mapping snow depth from manned aircraft on landscape scales at centimeter resolution using structure-from-motion photogrammetry. The Cryosphere 9, 1445-1463.

Pallister, J.S., Diefenbach, A.K., Burton, W.C., Muñoz, J., Griswold, J.P., Lara, L.E., Lowenstern, J.B., Valenzuela, C.E., 2013. The Chaitén rhyolite lava dome: Eruption sequence, lava dome volumes, rapid effusion rates and source of the rhyolite magma. Andean Geology 40, 277-294.

Ryan, G., Loughlin, S., James, M., Jones, L., Calder, E., Christopher, T., Strutt, M., Wadge, G., 2010. Growth of the lava dome and extrusion rates at Soufrière Hills Volcano, Montserrat, West Indies: 2005–2008. Geophysical Research Letters 37.

Sahetapy-Engel, S.T., Harris, A.J., Marchetti, E., 2008. Thermal, seismic and infrasound observations of persistent explosive activity and conduit dynamics at Santiaguito lava dome, Guatemala. Journal of Volcanology and Geothermal Research 173, 1-14.

Spampinato, L., Calvari, S., Oppenheimer, C., Boschi, E., 2011. Volcano surveillance using infrared cameras. Earth-Science Reviews 106, 63-91.

Stevenson, J.A., Varley, N., 2008. Fumarole monitoring with a handheld infrared camera: Volcán de Colima, Mexico, 2006–2007. Journal of Volcanology and Geothermal Research 177, 911-924.

Voight, B., 2000. Structural stability of andesite volcanoes and lava domes. Philosophical Transactions of the Royal Society of London A: Mathematical, Physical and Engineering Sciences 358, 1663-1703.

Wackrow, R., Chandler, J.H., 2008. A convergent image configuration for DEM extraction that minimises the systematic effects caused by an inaccurate lens model. The Photogrammetric Record 23, 6-18.

Wadge, G., Voight, B., Sparks, R., Cole, P., Loughlin, S., Robertson, R., 2014. An overview of the eruption of Soufriere Hills Volcano, Montserrat from 2000 to 2010. Geological Society, London, Memoirs 39, 1-40.

Zhang, C., Chen, T., 2001. Efficient feature extraction for 2D/3D objects in mesh representation, Image Processing, 2001. Proceedings. 2001 International Conference on. IEEE, pp. 935-938.

Highlights

- We apply structure from motion to oblique thermal images of Volcán de Colima
- Dome geometry between 2013 and 2015 is reconstructed at monthly intervals
- These models are compared to visible-light equivalents and found to correspond well
- The thermal models were more robust to degassing and poor lighting
- Thermal photogrammetry provides a useful additional tool for volcano monitoring